

LASER INTERFEROMETER GRAVITATIONAL WAVE OBSERVATORY  
- LIGO -

=====  
LIGO SCIENTIFIC COLLABORATION

Technical Note

LIGO-T2300137-v2

2023/08/13

## Report from the Heavy Suspension Workshop @ MIT

Edgard Bonilla, Brian Lantz, Lisa Barsotti, Craig Cahillane, Peter  
Fritschel, Oliver Gerberding, Evan Hall, Giles Hammond, Marie  
Kasprzack, Jeff Kissel, Kevin Kuns, Alexandra Mitchell, Eduardo Sanchez,  
Brett Shapiro, Calum Torrie, Betsy Weaver

*Distribution of this document:*

Public Document

<http://www.ligo.org/>

# Contents

<b>1</b>	<b>Introduction</b>	<b>5</b>
<b>2</b>	<b>Timeline</b>	<b>5</b>
<b>3</b>	<b>Requirements</b>	<b>6</b>
<b>4</b>	<b>Simple view of the BHQS and Reaction Chain</b>	<b>7</b>
<b>5</b>	<b>High stress fibers and Thermal noise</b>	<b>8</b>
<b>6</b>	<b>Table of Workshop Parameters</b>	<b>9</b>
<b>7</b>	<b>Installation</b>	<b>11</b>
<b>8</b>	<b>Design of the Main Chain</b>	<b>11</b>
8.1	Main Chain design constraints, heuristics, and tradeoffs . . . . .	11
8.2	Main Chain design logic . . . . .	13
8.3	Action items for main chain design . . . . .	14
<b>9</b>	<b>Design of the Reaction Chain</b>	<b>15</b>
9.1	Action items: . . . . .	16
<b>10</b>	<b>Local Sensing</b>	<b>17</b>
10.1	Introduction . . . . .	17
10.2	Local sensing requirements . . . . .	17
10.3	Deep-Frequency Modulation Interferometry sensors . . . . .	18
10.4	“Hamburg-style DFMI”: Balanced detection optical sensor heads “COmpact Balanced Readout Interferometers” (COBRIs) and parameter extraction using all signal harmonics . . . . .	18
10.5	Homodyne Quadrature Interferometers (HoQIs) . . . . .	19
10.6	Other Sensing Choices . . . . .	19
10.7	Actions . . . . .	20
<b>11</b>	<b>Actuation</b>	<b>20</b>

11.1 Magnet-Coil Actuators . . . . .	21
11.2 Electrostatic Drive (ESD) . . . . .	22
11.3 Photon Actuator . . . . .	22
<b>12 ASC</b>	<b>23</b>
<b>13 Test Mass Shape</b>	<b>24</b>
<b>14 Thermal Compensation</b>	<b>25</b>
<b>15 Modal Dampers</b>	<b>25</b>
<b>16 Conclusions</b>	<b>26</b>
<b>References</b>	<b>27</b>

## List of Figures

1	Notional timeline for A <sup>#</sup> development, from LIGO-G2300251. . . . .	6
2	Simple side view of the Heavy suspension main chain, reaction chain, and sensing and actuation, from G2301049 . . . . .	7
3	CAD sketch of the large optics in a BSC with the current Arm Cavity Baffle (left) and Transmission Monitor (right). From LIGO-D2300132-v6 . . . . .	8
4	Thermal noise estimate for the 100 kg optic suspended by 4 fibers stressed at 1.6 GPa, adapted from LIGO-T2300124. . . . .	9
5	Sensor and ISI motion drivers of the BHQS length. All the noises are below the 6e-12 m/rtHz noise requirement at 10 Hz (The green star). The largest drivers are the OSEM noise and the motion of the ISI coupled through the HoQI. From LIGO-G2301049. . . . .	16
6	Sensor measurements in the long degree of freedom on the AEI beamsplitter suspension when mounted onto the AEI-SAS seismic isolation table. Here, the OSEMS measure the top mass, the HoQIs measure the intermediate mass and the L4Cs are on the AEI-SAS table. . . . .	20
7	Advanced LIGO quadruple pendulum sensors and actuators for each stage, from Figure 10 of [17]. The main chain supports the test mass, while the reaction chain is used to mount the wired side of the actuators. OSEMs are “optical sensor and electro-magnetic actuators”, or coil drivers with magnets glued on the main chain. BOSEMs (“Birmingham Optical Sensor and Electro-Magnetic actuator”) were designed by the University of Birmingham, and have more actuation strength than AOSEMs (“Advanced LIGO Optical Sensor and Electro-Magnetic actuator”). . . . .	21

## 1 Introduction

On March 23 & 24, 2023, we convened a workshop at MIT to discuss the design of a suspension to support the 100kg optic which is planned for the LIGO A<sup>#</sup> upgrade. The goal was to establish the basic parameters for a new suspension so that the team could have a common understanding of the design which would allow us to move forward with various calculations, design concepts, and technology development. The design is based on the Advanced LIGO Quadruple Suspension, a suspension with a long and successful history. A set of upgrades to that design were presented and discussed, these were meant to address issues such as improving our ability to install suspensions quickly, improve the control noise and overall controllability of the suspension, lower the bounce and roll modes of the final optic, simplify the management of various resonances of the optic and fibers, and understand how to integrate the larger, heavier system into the existing space and weight constraints of the LIGO system and seismic isolation platforms.

This document lays out a set of “workshop parameters” for the new BSC Heavy Quadruple Suspension “BHQS”. These parameters provide a common starting point design consideration and baseline reference for calculations and optimizations which are required as we move to a conceptual design.

During O3, the noise of the Alignment Sensing and Control (ASC) loops was a significant source of low frequency (10–20 Hz) noise limiting the Differential ARM (DARM) length measurement - the main gravitational-wave readout channel. Modeling ASC and updating the suspension design to reduce the noise of the ASC control loops was a major topic of discussion at the workshop. This document attempts to capture the connections between the suspension design and the ASC control noise as a motivator for some of the design updates.

## 2 Timeline

On Jan 4, 2023, the LSC Council approved the recommendation to adopt A<sup>#</sup> as the next upgrade to the LIGO detectors [1]. In the current run plan, the A+ detectors will be taking data during the O4 and O5 runs, with O5 scheduled to last until the end of 2029. In order to begin installation of the A<sup>#</sup> right after O5 ends, a conceptual design, with accurate costing, needs to be complete before the end of 2024 so that a proposal to fund A<sup>#</sup> can be submitted in 2025 [LIGO-G2300251](#). In order to be considered for a project proposal, the suspension technology for A<sup>#</sup> should be at least a Technical Readiness Level (TRL) 6, “System/ Subsystem model or prototype demonstration in a relevant environment.” At the workshop, it was clear that many desirable pieces of the improved technology required for the A<sup>#</sup> suspensions, such as interferometric replacements for the local sensors, updated actuator configurations, and precision wire mounting technologies, are not yet at TRL 6 level (see TRL assessment in [LIGO-T2200287](#)). Getting the overall design and all of the necessary components to TRL 6 in the next two years is a critical task for the LSC.

Approximately one year is typically needed to secure funds. Therefore, by submitting a proposal in early 2025, and assuming that preliminary and final designs can be completed

supported by the LIGO Lab R&D funds and the LSC, the production units can be procured at the end of 2026 / beginning of 2027. This notional timeline leaves approximately two years available for assembling and testing the suspension units before installation (see figure 1). A bottom-up schedule for these tasks has not yet been done.

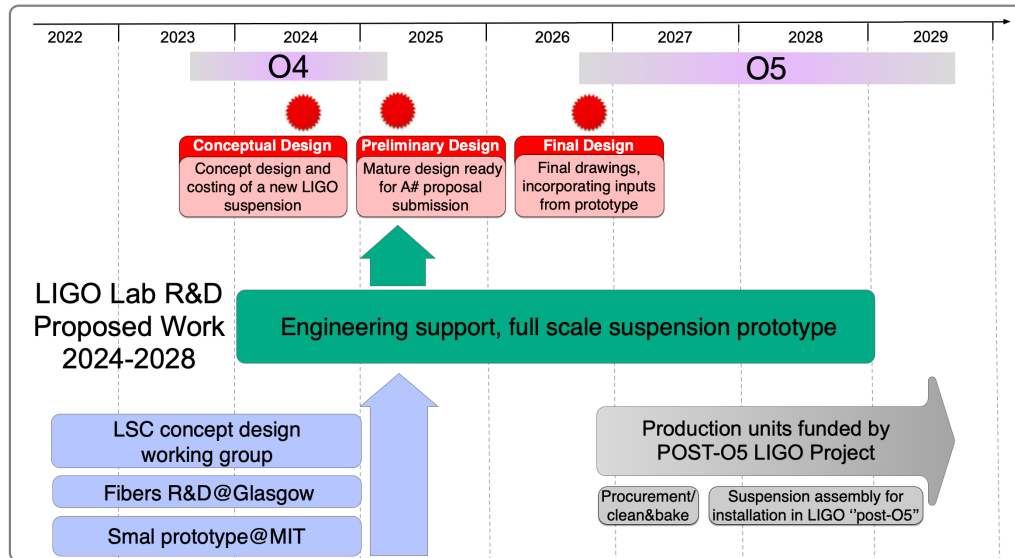


Figure 1: Notional timeline for A<sup>#</sup> development, from LIGO-G2300251.

### 3 Requirements

The final requirements for the A<sup>#</sup> suspensions have not yet been set, but this describes our working requirements. The suspension will be the same length as the aLIGO suspension, but it will be much heavier and occupy a larger footprint on the ISI optical table. A discussion of the requirements can be found in LIGO-G2300806 by Peter Fritschel.

There are several key requirements which are relevant to the BHQS design process:

- The optic will be about 100 kg, as described in the [Post-O5 report](#) [2] defining the A<sup>#</sup> program. Heavier masses provide better performance against radiation pressure, thermal noise, and Sigg-Sidles instability. The optic mass is limited to about 100 kg by the ability to procure the glass substrate, the ability to coat the mirror at LMA, and the isolation performance given an estimated total main chain mass of 400 kg.
- The total mass of the main suspension chain will be 400 kg. The 400 kg is an estimate of the maximum main chain payload given the current BSC-ISI payload limits. See [LIGO-G2300692](#) by Calum Torrie on the payload estimates.
- The longitudinal motion at 10 Hz should be less than  $6 \times 10^{-20} \text{ m} / \sqrt{\text{Hz}}$  at 10 Hz. This is set by the thermal noise. This is a bit higher than the current thermal noise estimate, see figure 4.

- The contributions to the length motion by other sources are still in discussion. Making all of the ‘technical’ noise sources  $10\times$  less than the main requirement is an excellent target, but may not be achievable, in particular for the ASC noise at high power.
- For modeling of the angular controls, we use a coupling of  $10^{-3}$  m/rad for angular to length coupling. This is similar to the current coupling in Advanced LIGO. The expected coupling is somewhat less than this. Understanding the current coupling is very important, and it is an active topic of investigation.
- The angular motion of the mirrors under ASC control should be less than  $10^{-9}$  rad RMS.
- The length of the suspension will not change (ISI table to beam height). The beam height will be the same as aLIGO, and the ISI optical table is not expected to move. There may be technical reasons to move the ISI table up a little bit (e.g. to improve access, or to simplify cartridge installation) but the suspension performance does not seem to require this.

## 4 Simple view of the BHQS and Reaction Chain

(Edgard B, Brian L)

The system described at the workshop is a quadruple suspension with a double reaction chain, see figure 2. The distance from the optical table down to the center of the optic is the same as for the Advanced LIGO test mass suspensions (roughly 1.62 meters). The size of the stages has increased substantially as described in section 6. The reaction chain is discussed in section 9, the design of the reaction chain is under discussion.

A simple CAD view of the bottom 2 stages of the main chain and reaction chain is shown in figure 3. It is clear from this view that fitting all of the components into the BSC chamber will be a challenge.

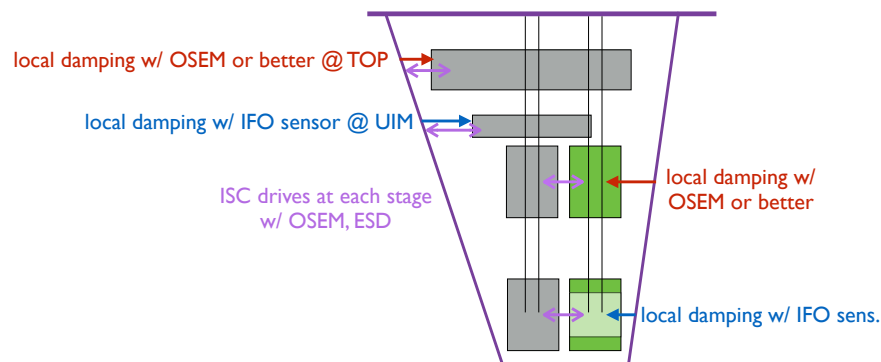


Figure 2: Simple side view of the Heavy suspension main chain, reaction chain, and sensing and actuation, from G2301049

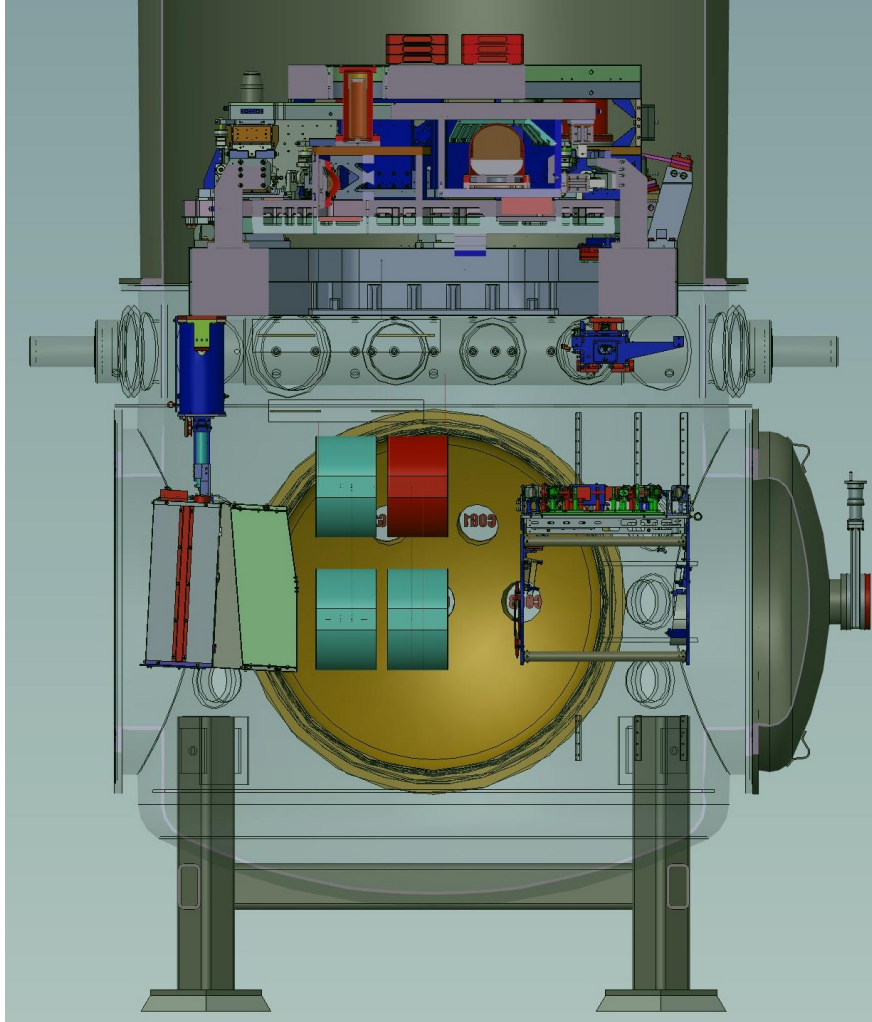


Figure 3: CAD sketch of the large optics in a BSC with the current Arm Cavity Baffle (left) and Transmission Monitor (right). From [LIGO-D2300132-v6](#)

## 5 High stress fibers and Thermal noise

The thermal noise of the suspension is extremely important. Fortunately, the manufacture of fused silica suspensions is well developed and the modeling for the thermal noise is well understood [3]. The suspension thermal noise of Advanced LIGO is very low, and the noise for A<sup>#</sup> should be even lower. The current expectation, as set forth in the [Post-O5 report](#) [2], is to support the bottom mass with glass fibers operating at 1.6 GPa of tensile stress. This is twice the stress used for the Advanced LIGO fibers. The Univ. of Glasgow has been conducting extensive development of higher stressed fibers, see for example [LIGO-T2300124](#) and [LIGO-G2200421](#) [4, 5]. The high-stress fibers have 3 benefits. First, the suspension thermal noise at 10 Hz is decreased to about 6e-20 m/rtHz at 10 Hz, as shown in figure 4. Second, the highest bounce and roll modes of the suspension can both be set below 10 Hz because of the higher compliance of the fibers. Third, the violin mode frequencies are increased because of the increased tension/ mass of the fibers.



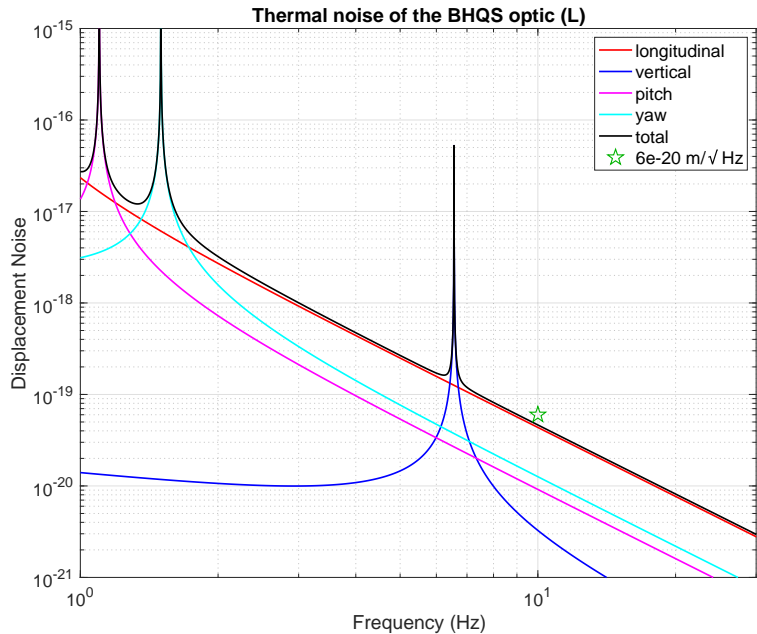


Figure 4: Thermal noise estimate for the 100 kg optic suspended by 4 fibers stressed at 1.6 GPa, adapted from LIGO-T2300124.

Research on the high-stress fibers is ongoing. It is critical that the life time, manufacture, and handling of these fibers be well understood.

Actions:

- Study the lifetime of fibers at 1.6 GPa, both in air and in vacuum.
- Study impact of short, higher-stress fluctuating forces on fiber lifetime.
- Check the calculations for pitch and yaw thermal noise.
- Develop weld tooling for A<sup>‡</sup>.
- Explore ways to speed up the weld and installation process
- Weld fibers with the Acoustic and Violin mode dampers (AMD, VMD) in place.
- look at ear design with larger area (horns) for welding.

## 6 Table of Workshop Parameters

Here we document the basic parameters of the BHQS presented at the workshop LIGO-T2300163[6]. Edgard Bonilla used these to develop a dynamics and control model of the Heavy Suspension using an updated version of the aLIGO suspension model he developed with Mark Barton. The model is available in the Suspension SVN, see [7] for details. This model is intended as a reference to enable control development and design comparisons. There are several important differences between the BHQS and the aLIGO suspensions - the design choices are discussed in section 8. In particular, the BHQS has 4 springs and wires supporting the top mass, all the wires are vertical, and the wire attachment points are

aligned (vertically) with the center of mass of the stage they are attached to.

Symbols	Description	TOP	UIM	PUM	TST
$m_n/m_1/m_2/m_3$	Mass (kg)	117	83	100	100
$I_{n,x}/I_{1,x}/I_{2,x}/I_{3,x}$	Roll moment of inertia ( $\text{kg}\cdot\text{m}^2$ )	8.1	3.6	2.6	2.6
$I_{n,y}/I_{1,y}/I_{2,y}/I_{3,y}$	Pitch moment of inertia ( $\text{kg}\cdot\text{m}^2$ )	8.1	3.3	1.9	1.9
$I_{n,z}/I_{1,z}/I_{2,z}/I_{3,z}$	Yaw moment of inertia ( $\text{kg}\cdot\text{m}^2$ )	15.5	6.7	1.9	1.9
$I_{n,xy}/I_{1,xy}/I_{2,xy}/I_{3,xy}$	R-P cross moment of inertia ( $\text{kg}\cdot\text{m}^2$ )	0	0	0	0
$I_{n,yz}/I_{1,yz}/I_{2,yz}/I_{3,yz}$	P-Y cross moment of inertia ( $\text{kg}\cdot\text{m}^2$ )	0	0	0	0
$I_{n,zx}/I_{1,zx}/I_{2,zx}/I_{3,zx}$	Y-R cross moment of inertia ( $\text{kg}\cdot\text{m}^2$ )	0	0	0	0
$k_{cn}/k_{c1}/k_{c2}$	Vertical spring stiffness (per side) (kN/m)	7.2	6.5	3.6	N/A
$k_{xn}/k_{x1}/k_{x2}$	Lateral spring stiffness (per side) (kN/m)	$\infty$	$\infty$	$\infty$	N/A
$Y_n/Y_1/Y_2/Y_3$	Young's moduli of wires (GPa)	$\infty$	$\infty$	$\infty$	72
$l_n/l_1/l_2/l_3$	Stretched wire length (m)	0.34	0.34	0.34	0.60
$r_n/r_1/r_2/r_3$	radii of wires ( $\mu\text{m}$ )	N/A	N/A	N/A	220
$d_{\text{top}}/d_n/d_1/d_3$	(upper) wire vertical attach offset (mm)	0	0	0	0
$d_m/d_0/d_2/d_4$	(lower) wire vertical attach offset (mm)	0	0	0	0
$s_n/s_u/s_i/s_l$	front-back wire separation (cm)	16	14	12.5	2.5
$n_{n0}/n_0/n_2/n_4$	(upper) wire transverse separation (cm)	18	13.5	23	23
$n_{n1}/n_1/n_3/n_5$	(lower) wire transverse separation (cm)	18	13.5	23	23

Table 1: BHQS parameters in QUAD notation [8].

Degree of freedom	Units	$f_1$	$f_2$	$f_3$	$f_4$
Longitudinal	[Hz]	0.45	0.96	1.8	2.6
Transverse	[Hz]	0.45	0.96	1.8	2.6
Vertical	[Hz]	0.6	1.8	2.9	6.2
Roll	[Hz]	0.59	1.45	2.4	8.7
Pitch	[Hz]	0.5	0.93	1.45	2.0
Yaw	[Hz]	0.6	1.1	1.5	2.8

Table 2: Resonant frequencies for BHQS

## 7 Installation

All new or upgraded BSC suspensions will be installed via the baseline “cartridge” scenario, unless further vacuum volume upgrades provide opportunities for easier installation development. This decision is driven by the desire to speed up the installation of new optics and is described in [LIGO-G2300692](#). This cartridge scenario involves removing the ISI from the chamber and mounting all new equipment to it while it is on a test stand near the chamber. The ISI will then be craned back into the chamber via the top chamber dome opening, with all of the new/upgraded suspension(s) parts mounted to it. The overall height of any new suspension(s) shall be designed such that there is adequate space to crane the cartridge over the chamber dome flange.

Tooling to handle all aspects of optic maneuvers and installation steps should be planned and designed concurrent with the design phase of the suspension(s). Scenarios for later plans of swapping the test masses, test mass cleaning, baffle installation, damper installation, and fiber failures should also be developed concurrent with designing the suspension(s) with an effort to minimize open-chamber time. Assembly and pre-installation areas for larger and or heavier suspensions at the sites will need to be revisited. Mechanical Test Stand loading for the new cartridge payload will need to be revisited.

There is also consideration of testing of the suspension prior to installation. This might be simple tests to confirm that the sensors and actuators are functioning, or perhaps tests in a small vacuum chamber to evaluate performance and measure the frequencies and Q’s of violin modes, etc.

## 8 Design of the Main Chain

The main drivers for the design of the main chain are to lower the control noise which impacts DARM. The main sources of this noise are the local damping of the suspension and the global angular sensing and control (ASC) of the interferometer (which controls the mirrors). By reducing the excitation of the mirror (particularly in angle) and reducing the natural modes of the suspension, the bandwidth of these loops can be reduced which lowers the noise in DARM at 10 Hz and above. Reducing the natural frequencies helps isolate the mirrors from all of these effects. Reducing the length-to-angle cross-coupling reduces the angular excitation of the mirrors. Reducing the cross-coupling also simplifies the design of higher performance controllers. The design thinking and the performance benefits are discussed in [LIGO-G2300701](#) and [LIGO-G2300711](#) [9, 10].

Many of the workshop design decisions were made according to the list of constraints and wishes that we itemize below.

### 8.1 Main Chain design constraints, heuristics, and tradeoffs

First, we list the ‘hard’ design constraints. These correspond to things that would be extremely hard to change or we simply do not wish to modify because it would impact other suspension performance or other parts of the LIGO system. These constraints are unlikely

to change in future iterations of the design. These are discussed in section 3, Requirements. The shortlist of hard design parameter constraints is:

- Test mass must be 100 kg.
- Total mass must be 400 kg.
- Fused silica test mass and supporting fibers.
- All resonant modes must be below 10 Hz.

Second, we list ‘semi-hard’ constraints. These correspond to things that we would prefer to keep in the design unless they result in significant performance improvements.

- Length of the suspension is the same as in aLIGO,  $L_{\text{tot}} = 1.62$  m.  
**Reason:** avoid moving the ISI.
- The suspension is a quadruple suspension.  
**Reason:** minimum number of stages to meet seismic isolation requirements without increasing the length.
- No resonances should be below 0.45 Hz.  
**Reason:** prevent the microseism from ringing suspension modes.
- Penultimate mass must be made of fused silica.  
**Reason:** sapphire is the only other reasonable choice in terms of thermal noise. A sapphire PUM can reduce the roll mode by 7% with respect to a silica one of the same mass. Not worth the effort.

Third, we list some preferences and heuristics used for the design. All of these are (and should) be up for discussion.

- Decouple the length and angular plants as much as possible, using four wires at the top, straight wires and aligned inertias.  
**Pros:** Better able to control the system with SISO loops. Less need to create filters to decouple a highly cross coupled plant. Simplified dynamics mean we can try sophisticated controls more successfully.  
**Cons:** Unable to use cross-coupled modes to reduce motion a-la Jeff Kissel’s level 2 damping [11]. Higher resonance for the pitch resonances. Pitch of the ISI will couple more strongly to the suspension below the first suspension pitch mode (0.45 Hz) compared to the current QUAD.
- Lower the end frequency edge of the ‘resonance forest’ of the suspension by better distributing masses and inertias. This leads to ‘top heavy’ suspensions, with lots of inertia at the top [12].  
**Pros:** Better 10 Hz isolation. More margin to roll off controllers.  
**Cons:** Lower visibility of modes at the top. UIM damping is recommended to properly damp resonances. This claim must be investigated.

- Increase the SNR of angular sensors by increasing the footprint of the upper masses. This also has some robustness effects.  
**Pros:** Stiffer and heavier top mass, harder to tip. Better angular sensing. Lower fractional change on stiffness/inertias due to imperfections.  
**Cons:** Larger footprint means we need to figure out what to do with the transmon. Unable to fit a four-stage reaction chain.
- Suspension fibers should be stressed at 1.6 GPa.  
**Tradeoff:** This is as much stress as currently seems achievable, see section 5. More stress on the fibers would simplify many design decisions. It would give higher violin mode frequencies and lower bounce/roll modes, which are both desirable.
- 100 kg PUM, same as the test mass.  
**Pros:** Lowers the bounce and roll modes as much as possible.  
**Cons:** Less longitudinal isolation and higher longitudinal modes compared to a lighter PUM.
- Test mass aspect ratio is the same as aLIGO.  
**Pros:** Unclear. Parametric instability? Newtonian coupling?  
**Cons:** Lowest pitch/yaw inertia for given mass. The Sigg-Sidles effect is stronger for lower moments of inertia [13, 14]. Likely harder to do thermal compensation compared to a mass with a smaller radius.
- Set minimum resonance frequencies for different modes. Vertical = 0.6 Hz, Pitch = 0.5 Hz, Yaw = 0.6 Hz.  
**Tradeoff:** Lowering the first vertical mode means larger blade springs. Lowering the pitch and yaw modes increases the interaction with the Sigg-Sidles effect.

## 8.2 Main Chain design logic

The following is the sequence of steps we followed to set the workshop parameters for the BHQS.

1. We assume the wire attachments are aligned vertically with the center of mass of the respective masses to decouple the angular degrees of freedom.
2. We set the masses of the PUM and the test mass to both be 100 kg, as previously discussed. For a given total length of the suspension, we can select the masses of the TOP and UIM following LIGO-T2100287 [12] to achieve best isolation at 10 Hz.
3. The length of the last stage was chosen to match the current length of 60 cm. 46 cm is the minimum distance possible due to the aspect ratio of the test masses.  
**Tradeoff:** Longer last stage lowers the bounce/roll modes, but impacts the longitudinal isolation. The best for longitudinal isolation is to make all lengths equal. Longer stage means easier access for violin mode sensors, but lower violin mode frequencies.
4. The lengths of the rest of the stages were chosen to maximize the longitudinal isolation following LIGO-T2100287 [12].

5. We find the blade spring stiffnesses which give the best 10 Hz vertical isolation. This is constrained by the requirement on the lowest vertical mode, and the mass of the upper stages.
6. We find the pitch/yaw torsional stiffnesses and inertias in the same way as the vertical calculation. The result of optimizing the isolation can be summarized as: use as much moment of inertia as possible and select the stiffnesses to meet the requirements. We then selected the baseline footprint of Figure 3 (also found in LIGO-D2300132-v6) assuming the top mass and UIM were made as aluminum boxes with 2 cm thick sides. **Tradeoff:** A large footprint means no space for a four stage reaction chain, and means the transmon must be moved or redesigned. More space is available for sensors, and the large separation gives better signal-to-noise ratio for angle measurement and gives more robustness against small imperfections. The aspect ratios of the upper masses must not be so extreme that their flexible modes become problematic.
7. The pitch and yaw rotational stiffnesses determine the location of the blade spring tips.
8. The roll plant is automatically determined from the pitch/yaw and vertical calculation for a given footprint.
9. We confirm that all the minimization steps lead to good enough isolation performance. However, both top mass and UIM damping might be required to meet the controls noise requirement specifications. **Tradeoff:** Designing to separate the suspension modes from the detection band gives us margin to roll off damping controllers, but it also limits the controllability and observability of modes at the top. The stiffer and heavier upper stage means that the top mass sees more of the high-frequency modes compared to the lower frequency modes of oscillation.

### 8.3 Action items for main chain design

- One proposed alternative is to work with the minimal possible rotational stiffness instead and determine the moments of inertia to satisfy the constraints, therefore revising steps 6-8 of the preceding logic.
- Explore the impact of moving/redesigning the transmon.
- Improve the generation of controllers to directly assess the impact of design changes on controls in lieu of using heuristics.
- Assess the interplay of the design with the LSC and ASC loops.
- Evaluate what limits the performance of the design - this is useful to drive additional research and to guide the Cosmic Explorer concepts.
- Study the precision of the wire attachments. This will limit the cross-coupling.
- Test design features (with prototypes and dedicated tests of particular pieces) to understand how well the decoupling can work.

## 9 Design of the Reaction Chain

At the workshop, Brian Lantz suggested that the reaction chain should have just 2 stages (LIGO-G2300686[15]). Estimates show that the simplified reaction chain meet the performance requirements for actuation of the test mass. We identified three drivers for the reaction chain design:

- Quiet location for the actuation.
- Quiet location for the local control sensors.
- Manage the back-reaction forces on the ISI from SUS actuation

We are considering a simpler reaction chain for several reasons. First, the large size of the top 2 stages of the workshop suspension means that the back surface of the optic and the back surface of the top stages are not aligned as they are in Advanced LIGO; this significantly complicates the design of a 3 or 4 stage reaction chain. Second, the payload of the ISI is limited and reducing the mass of the reaction chain eases the payload considerations. Finally, we note that none of the Advanced LIGO triple suspensions have a reaction chain. The triple reaction chains were all eliminated for Advanced LIGO (see LIGO-T020059 [16]), which reduced the size, weight, cost, and complexity of the system. We are not aware of any downsides resulting from that decision, except that the reaction force of driving the beamsplitter from the middle mass with no reaction chain disturbs the ISI during lock acquisition. Actuation disturbance forces must be considered for the BHQS design, but they are expected to be small.

If we consider the static electrostatic coupling from the ESD to be the main factor imposing requirements on the end reaction chain, the required motion for the reaction mass is  $7 \times 10^{-13}$  m/ $\sqrt{\text{Hz}}$  at 10 Hz. For reference, the ISI can achieve about  $10 \times 10^{-13}$  m/ $\sqrt{\text{Hz}}$  at 10 Hz. Therefore, from this perspective we barely need any isolation, and a two stage suspension is more than sufficient.

The proposed reaction chain is a double suspension.

**Pros:** The dynamics are simpler than a quadruple suspension, leading to lower resonance frequencies and simpler controls. A double suspension to reduce high frequency kicks to the ISI should be adequate.

**Cons:** The motion of the reaction point for the actuation points is larger - but the increase in noise seems negligible. The motion for the mounting point of the UIM sensors is larger. This is probably the largest noise source for the suspension, but it seems manageable.

Brian originally proposed attaching the reaction chain to an intermediate point in the suspension cage. However, it was agreed that suspending the reaction chain directly from the ISI is preferable, even though the suspension wires will likely pierce the top stage of the main chain, and the mounting of the top stage suspension springs will require some design thought to avoid interference. A sketch of the layout is shown in figure 2.

The motion of the masses is several orders of magnitude below the requirement set by the actuator coupling at 10 Hz - see figures in LIGO-G2300686. The biggest noise coupling at 10 Hz is the motion of the cage coupling through the back side of the sensors for the UIM, see figure 5 from LIGO-G223001049.



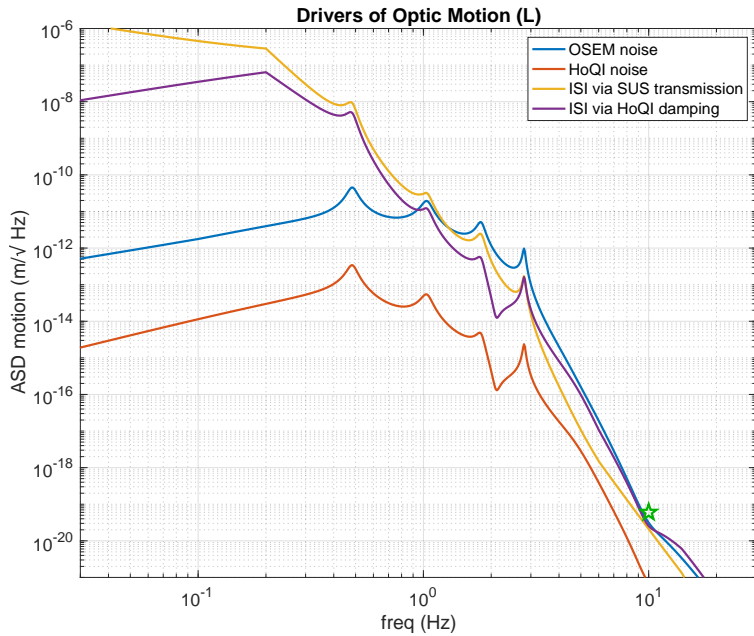


Figure 5: Sensor and ISI motion drivers of the BHQS length. All the noises are below the  $6e-12$  m/rtHz noise requirement at 10 Hz (The green star). The largest drivers are the OSEM noise and the motion of the ISI coupled through the HoQI. From [LIGO-G2301049](#).

There were several conversations about more innovative designs. These included integrating the reaction chain to the cage, hanging it from the UIM instead, making the reaction mass concentric with the test mass, and actuating the test mass against the PUM or UIM in a style similar to Virgo. These should be investigated, both for the A<sup>#</sup> design and for Cosmic Explorer.

### 9.1 Action items:

- Investigate the tradeoff between a double reaction chain and a triple in terms of the isolation of the UIM damping.
- Investigate how various designs of reaction chains impact the accuracy of main chain sensing. e.g. sensing the UIM w.r.t. a reaction chain has less noise at 10 Hz, but loss of absolute knowledge of the UIM position (because the reaction chain is moving) will impact the ability to do modal control.
- Make a short qualitative and quantitative tradeoff analysis for other reaction chain ideas.
- Establish the isolation requirements of the compensation plate.
- Check the dynamics of a double reaction chain hanging directly from the ISI.

2 masses is good enough for actuation noise, what about compensation plate? what about a quiet reference for the UIM sensing?



## 10 Local Sensing

OSEMs are drawn for the top mass. These should be upgraded. absolute sensing is needed for the top mass IFO sensing discussed for UIM gap sensing would be nice for lower stages Plan to have a Lab qualification/ bake-off at some point. Include optical levers- Michael Ross

Be sure to include where the sensors and actuators go on the stages. Violin modes.

### 10.1 Introduction

Local sensing for the A<sup>#</sup> suspension is an area of active research. The BHQS will need lower noise sensors than the OSEMs and sensing of the UIM to meet its performance targets for noise and for damping of the suspension modes. Several new sensors are in development, and others have been suggested. In addition to local damping of the suspension modes, several other control ideas were discussed which make use of better and more ubiquitous sensors.

### 10.2 Local sensing requirements

There are not yet any formal requirements for the local sensors. In part this is because they are being developed on a best-effort basis, so it's likely that a conceptual design will have 'performance targets'. Good sensors are defined by many characteristics, including

- Low noise, especially at 10 Hz.
- Compatibility with the LIGO vacuum and LIGO CDS control system.
- Reasonable range and reasonable standoff.
- Good stability, linearity, and calibration. Low cross-coupling.
- We need to know the location of the top mass w.r.t the cage for alignment, etc.
- It may be useful to know the gaps between the lower masses of the main chain and the suspension cage, the gaps between the reaction chain masses and the suspension cage, and the gaps between the main chain and the reaction masses.
- Wiring must be compliant enough that it doesn't compromise performance. For aLIGO, all wires are on the reaction chain. It may be possible to have wiring to the top mass of the BHQS main chain.
- Sensors must not compromise the thermal noise or environmental sensitivity of the chains (e.g. response to magnetic fields in the LIGO vacuum).
- There are several practical considerations such as ease of installation, long life, reasonable failure characteristics, etc.
- The actuators do not need to be integrated with the sensors.

**Actions:** Sensing requirements which are needed to aid the development of new sensors need to be developed as soon as possible. Requirements should be justified with respect to the final system to help avoid bad requirements.

### 10.3 Deep-Frequency Modulation Interferometry sensors

DFMI sensors are based on compact, unequal arm-length interferometers in combination with a strong laser frequency modulation (typically a modulation depth of a few GHz and a modulation rate of a few 100 Hz to 1 kHz). A single laser can supply multiple optical sensors that share the same laser-frequency noise within the measurement band, so it can either be actively controlled or subtracted in post-processing. The optical signals of DFMI sensors have a non-linear cosine of a cosine shape from which the relevant parameters can be extracted in multiple ways. Typically, the signal is demodulated by the modulation frequency and its harmonics and then processing is done on the complex harmonic amplitudes.

### 10.4 “Hamburg-style DFMI”: Balanced detection optical sensor heads “COBRIs” and parameter extraction using all signal harmonics

An optical sensor head design is investigated in Hamburg which uses polarisation to enable balanced detection (diodes at the direct and indirect port of a small Michelson). Thereby the influence of ghost beams in on-axis optical heads can be reduced, this should avoid the otherwise prominent non-linearity and we gain a factor  $\sqrt{2}$  in the noise floor. The optical head uses a 1 mm beam diameter to realize an angular sensing range simulated to be at least  $\pm 400 \mu\text{m}$  (See [LIGO-P2100022](#)) for a 5 cm distance to the test mass, but it can operate with much larger distances. First prototypes of these optical heads are currently being tested (see workshop presentation [LIGO-G2300717](#)). This work is based on previous in-vacuum results with compact DFMI sensors (see [PhysRevApplied.12.034025](#) and [Thesis by K.-S. I.](#)) that achieved a noise floor of  $2.3 \times 10^{-13} \text{ m}/\sqrt{\text{Hz}}$ , then limited by data acquisition noise. The white noise limit expected for COBRIs in combination with the optimal readout algorithm is  $> 9 \times 10^{-15} \text{ m}/\sqrt{\text{Hz}}$  (see [LIGO-P2100413](#))

The readout scheme investigated in Hamburg is based on using the information of all signal harmonics, which provides the optimal SNR and minimal readout noise possible (see [P2100413](#)), as well as absolute ranging information in the form of the modulation depth  $m$ . Since the algorithm works on almost arbitrary distances each sensor can have a different distance to the target. Originally, a non-linear fit algorithm was used to determine the phase in real-time (see [P2100022](#), [Thesis by K.-S. I.](#) and [DPM paper by Heinzl et al.](#)), but since it is computationally expensive a non-iterative algorithm was developed (see [G2300565](#) and [P2300078](#)) that is currently being tested in python and will be implemented on an FPGA system. In the scope of this work also the non-linearity induced by higher dynamics in the DFMI signals is being investigated and mitigated (see [G2300565](#)).

The following actions are necessary/planned:

COBRIs: Test COBRIs in vacuum, ideally on suspensions; implement COBRI with correct beamsplitter coating (see [G2201438](#)); commercialize COBRI production with vacuum compatibility.

Algorithm: Test the new algorithm with COBRIs, ideally on suspensions; finish algorithm implementation on FPGAs infrastructure at Hamburg; investigate integration of algorithm (on CDS or FGPAs) at LIGO; realise absolute ranging tests

Opto-electronics: will test laser amplifier to increase number of optical heads per laser; need

to identify suitable fiber (or free-beam) couplers to distribute the light with good polarisation extinction ratio and vacuum-compatibility (see [PhD Thesis by Katharina-S. I.](#)).

## 10.5 Homodyne Quadrature Interferometers (HoQIs)

HoQIs are compact interferometric sensors which use multiple readouts and birefringent elements to measure motion which is sub-wavelength. They have a published in-air measured noise performance of  $8 \times 10^{-14} \text{ m}/\sqrt{\text{Hz}}$  at 10 Hz (See [LIGO-P1700133](#)). Tests to demonstrate the in-vacuum noise performance have been inconclusive due to noisy electronics but these should be available in the near future. Their use has been demonstrated in multiple systems, most notably as the readout mechanism for the cylindrical rotation sensor (see [LIGO-G2300474](#)) and in measuring suspension test masses (see [LIGO-G2300934](#)). As they have been implemented in multiple LIGO systems at multiple locations including at Caltech, the AEI, University of Birmingham and University of Washington they have mature system and optomechanical integration.

For the BHQS the HoQIs would be used to measure motion of test masses in the suspension. This is a concept which has been demonstrated at the AEI 10m prototype in Hannover where three HoQIs are installed on the beamsplitter suspension measuring the intermediate mass. [Figure 6](#) shows a comparison of the sensors in the long degree of freedom. This shows that the OSEM cannot measure motion above 10 Hz but the HoQI can. A discussion point which came out of these graphs from the workshop is that the OSEM noise floor is very high. LIGO BOSEMs have a noise floor of around  $10^{-11} \text{ m}/\sqrt{\text{Hz}}$ , but these OSEMs were not made to LIGO specifications and have been shown to be noisier in previous tests at the AEI. Another discussion point was about the fact that the HoQIs and OSEMs see the same amplitude of motion below 10 Hz but they are measuring different masses. We believe this is because the sensors are measuring the difference between the test mass and the cage which the sensors are mounted to. Therefore, this motion comes from the transmission of residual table motion from the AEI-SAS to cage motion. Further work to show that the motion we see is table motion is being done by building a model of the suspension.

HoQI deployment on the BHQS requires modelling of the suspension and a comparison to the sensor noise to see whether they would be capable of sufficiently measuring motion. To do this better in-vacuum noise performance measurements need to be made to be used in the models. From this a ‘HoQI damping’ model can be made which would allow us to see the effect of using HoQI signals for damping of the masses. This can also be compared to other local sensors. The mechanical design might need to be modified for optimal mounting on the BHQS and improvements in the noise performance will be a continuous process.

## 10.6 Other Sensing Choices

We need to evaluate other sensing choices. Two ideas were mentioned - optical levers and compact inertial sensors in the top mass. Optical levers could be used to measure angular position and vibration for any of the stages. Compact inertial sensors could be placed inside the top mass and used to measure the motion at 10 Hz.

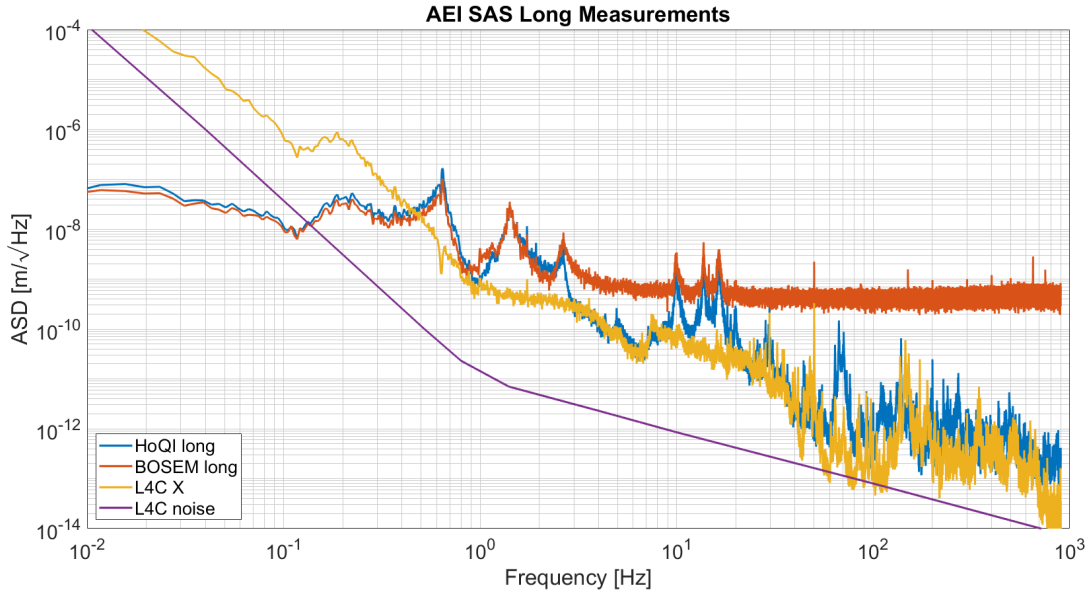


Figure 6: Sensor measurements in the long degree of freedom on the AEI beamsplitter suspension when mounted onto the AEI-SAS seismic isolation table. Here, the OSEMS measure the top mass, the HoQIs measure the intermediate mass and the L4Cs are on the AEI-SAS table.

## 10.7 Actions

- Development of local interferometric sensors should continue so they can be ready for A<sup>#</sup>.
- Requirements which are needed to allow sensor development should be identified and set..
- The LIGO Lab and LSC need to develop and evaluation and acceptance process for new sensors.
- A timeline for new sensors needs to be written. This should include when various performance targets need to be demonstrated.
- Uses and performance targets for other sensing choices needs to be established.

## 11 Actuation

The actuators must be increased in strength to accommodate the larger mass and moments of inertia of the heavy suspension. The DARM degree of freedom is currently controlled via the end test mass electrostatic drive (ESD) and the upper stages, although the top mass is not currently used. The arm angular degrees of freedom are controlled via the penultimate mass coil drivers. Additionally, actuators attached to the ISI are used to damp the suspension resonances as a part of the the damping control loops.

The actuators for each stage must be considered in the context of the entire suspension.

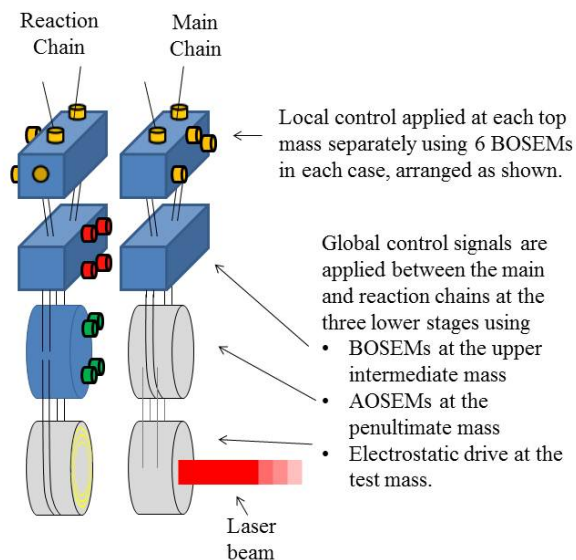


Figure 7: Advanced LIGO quadruple pendulum sensors and actuators for each stage, from Figure 10 of [17]. The main chain supports the test mass, while the reaction chain is used to mount the wired side of the actuators. OSEMs are “optical sensor and electro-magnetic actuators”, or coil drivers with magnets glued on the main chain. BOSEMs (“Birmingham Optical Sensor and Electro-Magnetic actuator”) were designed by the University of Birmingham, and have more actuation strength than AOSEMs (“Advanced LIGO Optical Sensor and Electro-Magnetic actuator”).

Actuator offloading is the process of allocating actuation force to upper stages of the suspension to alleviate demands on the lower stage actuators. Limitations to offloading are usually determined by the compliance of the suspensions stages: you can’t offload high-frequency actuation to upper stages because the suspension compliance falls away like  $1/f^2$  per stage.

A table of the current actuator parameters exists here: [18].

Below we overview the options and considerations for actuating the heavy suspensions. It would also be interesting to consider other geometries (also ask Bram and Jon Richardson, both ESD and Osems)

### 11.1 Magnet-Coil Actuators

The most common and simplest method of actuation on a suspended optic is the magnet-coil actuator. The magnet is epoxied to the back of the test mass, and a coil of wire is wound around the magnet and attached to the reaction mass. The maximum actuation strength is determined by the number of turns in the coil and the magnet strength. Coil actuators are packaged together with a shadow position sensor under the name OSEM [19]. Coil actuators are comparatively simple to install and align.

For the heavy suspensions, coil actuators will likely be used as the upper stage actuators again for the top stage, upper-intermediate stage, and penultimate stage. This is due to the versatility of the magnet-coil arrangement.

**Actions:**

- **Authority** How strong does each of the upper stages coil actuators need to be? This can be answered by looking at the LSC and ASC feedback to each stage, as well as the damping loop feedback to the top stage, and estimating the maximum range used during lock acquisition and low-noise operations.
- **Noise** Also important are the noise considerations: the noise from the actuators, and especially the digital-to-analog drivers, must fall below the expected DARM noise floor. The coils can be placed in “low-noise operation” once full lock has been achieved.
- **Actuator placement** We also need to consider the arrangement of the actuators, and the possibility of having different actuators for different degrees of freedom [20], because, for example, the vertical stiffness of the top stage is 14.5 kN/m while the pitch stiffness is only 380 N · m[6], so small cross-coupling from the vertical drive could excite significant pitch motion.
- **Coil Geometry** We should also consider geometries which are more sophisticated than a coil and a dipole magnet. Magnet-coil actuators often use flux returns to concentrate the field of the magnet to a well controlled region improving the efficiency and linearity of the actuator, and minimizing it’s interaction with other fields.

## 11.2 Electrostatic Drive (ESD)

An electrostatic drive uses the dielectric nature of the test mass substrate to actuate. A large bias voltage is placed on the reaction mass just 5 mm behind the test mass, creating a capacitive system between the reaction and test masses than can be used to control the test mass position.

The ESD is currently used to actuate on an end test mass to control DARM for O4. It satisfies both range and noise requirements lock acquisition and for low-noise operation at both sites. The ESD is also used to damp parametric instability modes [21].

It has been observed in the leadup to O4 at LIGO Hanford that grounding noise at the X-end appears in DARM [22], and that the grounding noise coupling is proportional to ESD bias [23–26]. While these sources of noise have been investigated thoroughly and mitigated, it is difficult to know if further improvements in voltage noise coupling through the ESD are possible.

## 11.3 Photon Actuator

A photon actuator is an auxiliary laser incident on the test mass front, which pushes on the test mass via radiation pressure. Currently, two photon actuators, known as “photon calibrators” or PCALs, are used at each site in order to calibrate the detector motion [27]. In 2016 at LIGO Livingston, the photon calibrator was used to control the differential arm length for a short time [28, 29].

A photon actuator should be investigated as a possible alternative to the electrostatic drive for both lock acquisition and low-noise operation. Advantages include the opportunity to remove the final stage of the reaction chain and the compensation plates, eliminating squeezed film damping noise, removal of high voltage nodes 5 mm behind the test mass, eliminating the potential for voltage noise and charge noise, and remote actuation from outside the chamber. Disadvantages include high power auxiliary laser requirements, thermal distortion of the test mass due to auxiliary laser, and undemonstrated ability to damp parametric instability modes in place of the ESD.

**Actions:**

- **Authority** How strong does the actuator on the test mass have to be to acquire lock?
- **Spot Positions** Can the auxiliary laser spot positions on the test mass be controlled with sufficient accuracy over a long period of time?
- **Thermal Effects** Will too much auxiliary laser power on the test mass deform the optical beam quality?
- **Parametric Instability Damping** The ESD is capable of damping PI modes. Can the photon actuator do the same?

## 12 ASC

The Alignment Sensing and Control (ASC) loops are a significant source of noise in the low frequency region of the detection band. The goal is to design a suspension that minimizes the angular noise contribution to DARM by reducing the angular excitation of the optic by reducing the cross-coupling from ISI length to angle, reducing the angular noise of the local sensors and actuators, reducing the bandwidth of the interferometer angular control loops, and reducing the coupling of angular control drive to DARM.

Some of the tasks for a heavy suspension hinge on understanding several effects in the current interferometers:

- Roughly speaking, the coupling factor of test mass angle fluctuations into DARM displacement is set by the rms level of beam spot motion [30]. Based on the observed noise level, this rms spot motion seems to be of order 1 mm. This was previously considered to be at odds with the calibrated in-loop angular error signals, which implied an rms spot motion about 10 times smaller; however, recent measurements using test mass cameras as out-of-loop witnesses indicate that a revised calibration might explain the observed rms spot motion (LLO:64562).
- To avoid point absorbers, LIGO currently runs with beam spot positions that are significantly displaced from the center of the test mass surface. A modeling task relevant for both A+ and A<sup>#</sup> is probabilistic (Monte Carlo) simulation of optomechanical angular plants to include this miscentering effect.

The question of choosing the A<sup>#</sup> test mass geometry for Sigg–Sidles effect is discussed in §13.

**Actions:**



- We need a good model to predict the control noise for ASC control on BHQS suspensions. This is a very high priority.
- We need to understand why the measured coupling of ASC to DARM is larger than the expected coupling.

## 13 Test Mass Shape

The shape of the test mass, especially its aspect ratio, are important when designing the dimensions of the suspensions, and there are several factors which must be considered when choosing the shape. These include minimizing the effects of the Sidles-Sigg radiation pressure induced angular instabilities, minimizing parametric instabilities, reducing the requirements placed on the thermal compensation system (TCS) needed to correct the effects of the high laser power in the arms, and the practicalities of manufacturing and coating the test masses. Simply scaling the dimensions of the LIGO test masses by a factor of  $(100/40)^{1/3}$  in each linear dimension results in a test mass with thickness 27 cm and radius 23 cm.

Radiation pressure acting between the test masses creates torsional springs which shift the free torsional modes of the suspensions. In one mode, the hard mode, the spring becomes stiffer and the resonance increases in frequency, while in the other mode, the soft mode, the spring is softened and the resonance decreases, possibly becoming unstable if the shift is large enough. The ultimate frequencies of these modes should be kept small so that the bandwidths of the angular control loops can be minimized. The shifts of the squared frequencies of these modes are  $\Delta(\omega)^2 \propto P/I$ , where  $P$  is the arm power and  $I$  is the moment of inertia. Scaling up each dimension by  $(100/40)^{1/3}$  minimizes the moment of inertia, thus maximizing the frequency shifts. However, even with the 1.5 MW maximum arm power planned for A<sup>#</sup> and this minimum moment of inertia, this corresponds to a squared frequency shift roughly 25 % less than that currently experienced at LHO with a maximum arm power of  $\sim 430$  kW. Thus, while the detailed locations of the suspension resonances are important, the magnitude of the shifts due to the Sidles-Sigg instabilities will not be a factor in determining the test mass shape, even if the soft mode becomes unstable.

The test mass shape also determines the frequencies and mode shapes of the acoustic modes of the test masses which interact with the higher order optical modes to produce parametric instabilities. The shape should thus be chosen such that the parametric gain, determined by these two factors, is small for as many modes as possible. In addition to the aspect ratio, the detailed shape, e.g. dimensions of the flats, is important in determining these gains. The gains can also be reduced by adding acoustic mode dampers (AMDs) to the test mass at locations which add sufficiently small thermal noise. The details of the AMDs should also be considered along with the determination of the test mass shape.

The aspect ratio of the test mass also influences how easy it will be to correct the thermal distortions with the thermal compensation system described in §14. We thus expect that TCS considerations will largely set the aspect ratio of the test mass while the detailed shape will be mostly determined by PI considerations. Simulations are ongoing to study both of these effects.

Another consideration is that the test mass must fit in the coating and polishing machines.



The maximum thickness that the current machines can handle is 20 cm, which is the radius of the 105 kg test masses that Virgo plans to use in O5. It is important to determine the prospects for increasing the thickness and to understand the limits to radius. The radius of a 20 cm thick 100 kg fused silica mass is 27 cm.

## 14 Thermal Compensation

This workshop did not go too far into the interplay between thermal compensation and heavier masses/suspensions, but several considerations can already be deduced:

- The mechanical design of the mass/suspension/cage needs to account for the presence of ring heaters, or any other irradiation apparatus such as FroSTI ([LIGO-G2300506](#)) that may be added. The location of the ring heater along the barrel of the test mass will be determined by the optimal distance needed to correct the combination of thermal lens and surface deformation for the chosen test mass geometry. In addition to the issue of space constraints, the mechanical design can affect the amount of sag, and hence optic misalignment, that results from changing the heater temperature.
- The test mass geometry should be chosen to give the smallest thermal time constants that are practical. The thermal timescale for applying ring heating to the current 40 kg optics is of order 1 day, which significantly constrains the ability to find a sensibly tuned thermal operating point for the interferometers in a finite amount of time. Conversely, the thermal timescale for the CO<sub>2</sub> laser heating of the compensation plates is of order 1 hour and is tolerable.
- The test mass geometry (and compensation plate geometry) affects the spatial profile of both the deformation induced by absorption of the main interferometer beam, as well as the corrective deformation induced by the thermal compensation system. (This deformation includes both surface deformation of the HR surface and optical path distortion from travelling through the substrate.) In addition to issues of how much spherical power is induced (and how much can be corrected), the severity of higher-order Zernike effects may lead us to prefer some test mass geometries over others.

## 15 Modal Dampers

The Advanced LIGO suspensions have been retrofitted with a variety of tuned mass dampers to help control various high-Q resonances which cause trouble for the interferometer. These include Acoustic Mode Dampers (AMDs) which help control parametric instabilities in the detector, Violin Mode Dampers (VMDs) which damp the modes of the glass suspension fibers, and Bounce/ Roll mode dampers (BRDs) which damped the modes of the optic and the PUM stretching the glass fibers. These dampers will be incorporated into the suspension design from the beginning, which will simplify the installation and allow improved access. There are some new ideas for the violin mode dampers which are being explored [31].

## Actions

- Redesign BRSs to allow better access.
- Update AMD design to cover more modes in high power operation.
- Develop and test alternate VMD designs.

## 16 Conclusions

The Heavy Suspensions workshop was successful in establishing requirements and a shared vision for the A<sup>#</sup> suspension. It will be closely based on the design history of the GEO600 and Advanced LIGO suspensions, although it will be significantly more massive, have higher stressed fibers, and have improved local sensors. Careful design to reduce cross coupling and reduce the frequency of the highest suspension modes should reduce the in-band (10 Hz and above) control noise, allowing the interferometer to reach thermal noise limits at 10 Hz.

The workshop parameters and models will allow coordinated development of the suspension and required components across the LSC. It is clear that significant work remains, and it is critical that these development efforts be coordinated and supported so that the an A<sup>#</sup> proposal can be submitted in 2025.

## References

- [1] S. Penn, *Agenda of the LSC Council, Jan 4, 2023*, [20230104Agenda](#) (cit. on p. 5).
- [2] P. Fritschel et al., “Report of the LSC Post-O5 Study Group”, [LIGO Document T2200287](#) (2022) (cit. on pp. 6, 8).
- [3] A. V. Cumming et al., “Lowest observed surface and weld losses in fused silica fibres for gravitational wave detectors”, [Classical and Quantum Gravity](#) **37**, 195019 (2020) (cit. on p. 8).
- [4] G. Hammond et al., “Heavy SUS at Glasgow (Thermal Noise)”, [LIGO Document T2300124](#) (2023) (cit. on p. 8).
- [5] K. Haughian et al., “Update on suspension and bonding activities at Glasgow”, [LIGO Document G2200421](#) (2022) (cit. on p. 8).
- [6] E. Bonilla and B. Lantz, “Summary of BHQS workshop parameters”, [LIGO Document T2300163](#) (2023) (cit. on pp. 9, 22).
- [7] E. Bonilla, *Full BHQS model posted*, [SWG alog 12068](#) (cit. on p. 9).
- [8] J. Kissel and M. Barton, *QUAD Pendulum Parameter Descriptions and Naming Convention*, tech. rep. (LIGO Internal Document T1400447, 2014) (cit. on p. 10).
- [9] J. Kissel, “Kissel’s List of Design Thoughts for the BHQS”, [LIGO Document G2300701](#) (2023) (cit. on p. 11).
- [10] E. Bonilla, “BHQS dynamics tradeoff notes”, [LIGO Document G2300711](#) (2023) (cit. on p. 11).
- [11] J. Kissel, “aLIGO QUAD ‘Level 2’ Damping Loop Design”, [LIGO Document G1300537](#) (2013) (cit. on p. 12).
- [12] E. Bonilla, “Calculations for optimal mass distributions in multi-stage suspensions”, [LIGO Document T2100287](#) (2021) (cit. on pp. 12, 13).
- [13] E. Bonilla, “Technical Note on BHQS Sigg-Sidles modes”, [LIGO Document T2300150](#) (2023) (cit. on p. 13).
- [14] K. Kuns, “Impact of A# Test Mass Geometry on Angular Instabilities”, [LIGO Document G2300704](#) (2023) (cit. on p. 13).
- [15] B. Lantz and E. Bonilla, “A# Reaction chain - requirements and use of a double suspension”, [LIGO Document G2300686](#) (2023) (cit. on p. 15).
- [16] N. Robertson et al., “Are Reaction Chains Needed for aLIGO HAM Optics?”, [LIGO Document T020059](#) (2002) (cit. on p. 15).
- [17] S. M. Aston et al., “Update on Quadruple Suspension Design for Advanced LIGO”, [Classical and Quantum Gravity](#) **29**, 235004 (2012) (cit. on p. 21).
- [18] J. Kissel, *Suspensions Controls Design Summary Table*, tech. rep. (2011), G1100968 (cit. on p. 21).
- [19] L. Carbone et al., “Sensors and actuators for the Advanced LIGO mirror suspensions”, [Classical and Quantum Gravity](#) **29**, 115005 (2012) (cit. on p. 21).

- [20] J. Kissel and B. Lantz, “Co-Designing the Post O5 Quadruple Suspension: Podcast Episode 1 – Controlling the Top Mass”, [LIGO Document G2102370](#) (2023) (cit. on p. 22).
- [21] C. Blair et al. (LSC Instrument Authors), “First demonstration of electrostatic damping of parametric instability at advanced ligo”, [Phys. Rev. Lett. 118](#), 151102 (2017) (cit. on p. 22).
- [22] R. Schofield, *95 hz peak reduced in esd power supply monitor; darm not yet checked*, [LHO alog 65907](#) (cit. on p. 22).
- [23] R. Schofield, *Ex ground noise coupling further reduced by new ground straps, and coupling is proportional to bias*, [LHO alog 66469](#) (cit. on p. 22).
- [24] R. Schofield, *Update on grounding noise studies*, [LHO alog 67075](#) (cit. on p. 22).
- [25] R. Schofield, *Grounding noise coupling at the corner station is low whenever itmx and itmy biases are similar, and coupling at low frequencies is less dependent on bias*, [LHO alog 67627](#) (cit. on p. 22).
- [26] R. Schofield, *Corner station grounding noise can be further reduced by setting biases to 0v (itmx), 60v (itmy) and by grounding ethercat chasis*, [LHO alog 68053](#) (cit. on p. 22).
- [27] S. Karki et al., “The Advanced LIGO photon calibrators”, [Rev. Sci. Instrum. 87](#), 114503–114503 (2016) (cit. on p. 22).
- [28] D. Martynov et al., *Locking tuning, darm on pcal, 65Hz scatter*, [LLO alog 28481](#) (cit. on p. 22).
- [29] S. Kandhasamy et al., *DARM actuation using PCAL*, [LLO alog 28500](#) (cit. on p. 22).
- [30] L. Barsotti, M. Evans, and P. Fritschel, “Alignment sensing and control in advanced LIGO”, [Class. Quant. Grav. 27](#), 084026 (2010) (cit. on p. 23).
- [31] S. Ballmer, “Electrostatic Violin Dampener Thoughts”, [LIGO Document G2300716](#) (2023) (cit. on p. 25).